How *Staphylococcus aureus* biofilms develop their characteristic structure

Saravanan Periasamy, Hwang-Soo Joo, Anthony C. Duong, Thanh-Huy L. Bach, Vee Y. Tan, Som S. Chatterjee, Gordon Y. C. Cheung, and Michael Otto[1]

National Institute of Allergy and Infectious Diseases, National Institutes of Health, Bethesda, MD 20892

Biofilms cause significant problems in the environment and during the treatment of infections. However, the molecular mechanisms underlying biofilm formation are poorly understood. There is a particular lack of knowledge about biofilm maturation processes, such as biofilm structuring and detachment, which are deemed crucial for the maintenance of biofilm viability and the dissemination of cells from a biofilm. Here, we identify the phenol-soluble modulin (PSM) surfactant peptides as key biofilm structuring factors in the premier biofilm-forming pathogen *Staphylococcus aureus*. We provide evidence that all known PSM classes participate in structuring and detachment processes. Specifically, absence of PSMs in isogenic *S. aureus psm* deletion mutants led to strongly impaired formation of biofilm channels, abolishment of the characteristic waves of biofilm detachment and regrowth, and loss of control of biofilm expansion. In contrast, induced expression of *psm* loci in preformed biofilms promoted those processes. Furthermore, PSMs facilitated dissemination from an infected catheter in a mouse model of biofilm-associated infection. Moreover, formation of the biofilm structure was linked to strongly variable, quorum sensing-controlled PSM expression in biofilm microenvironments, whereas overall PSM production remained constant to ascertain biofilm homeostasis. Our study describes a mechanism of biofilm structuring in molecular detail, and the general principle (i.e., quorum-sensing controlled expression of surfactants) seems to be conserved in several bacteria, despite the divergence of the respective biofilm-structuring surfactants. These findings provide a deeper understanding of biofilm development processes, which represents an important basis for strategies to interfere with biofilm formation in the environment and human disease.

Bacterial biofilms are sticky agglomerations of bacteria embedded in an ECM. Owing to their high resistance to mechanical interference, mechanisms of innate and acquired host defenses, and antibiotic treatment (1), they cause enormous problems in the environment as well as in human and animal infections. Biofilm-associated infections are characteristically chronic and frequently occur in hospitals. *Staphylococcus aureus* is a leading cause of such infections (2).

Bacterial biofilm formation proceeds in three steps: initial adhesion, proliferation, and detachment. Adhesion may occur onto virtually any biotic or abiotic surface. *S. aureus*, in particular, has an extraordinary capacity to attach to indwelling medical devices through direct interaction with the device's polymer surface or by establishing connections to human matrix proteins after those proteins have covered the device. Then, proliferation proceeds through the production of an ECM that contributes to intercellular aggregation. In staphylococci, the matrix consists of several secreted polymers such as exopolysaccharide, teichoic acids, and specific proteins as well as DNA originating from lysed cells (2).

The creation of a viable biofilm requires channels through which nutrients can penetrate into deeper biofilm layers and thus, additional factors that disrupt cell–cell interactions (3). These factors can, ultimately, also lead to the detachment of cells and cell clusters from the biofilm and therefore, control biofilm thickness and expansion. Biofilm detachment plays a critical role during biofilm-associated infection, because it enables cells to spread through the blood and other body fluids to new infection sites (2, 4). However, we have a lack of understanding about such biofilm-disruptive factors and their role in biofilm maturation and detachment processes.

In *S. aureus*, it is known that biofilm detachment is controlled by the quorum-sensing system Agr (5–7), but the quorum-sensing controlled molecular detachment factors of *S. aureus* remain undefined. Enzymes that degrade essential biofilm polymers may theoretically contribute to biofilm detachment; however, there is only preliminary evidence for such enzyme function in *S. aureus* or other staphylococci (7, 8). In contrast, there are reports indicating that several bacteria use surfactant-like molecules to structure and detach biofilms, which include *Bacillus subtilis* surfactin (9, 10), *Pseudomonas aeruginosa* rhamnolipid (11, 12), and the phenol-soluble modulin (PSM) β-peptides in *Staphylococcus epidermidis*, a close relative of *S. aureus* (4). Thus, there is growing evidence suggesting that quorum-sensing controlled expression of surfactant molecules is crucial to biofilm maturation processes.

PSMs are staphylococcal peptides with an α-helical, amphipathic structure, which gives them surfactant-like characteristics (13–15). They are genome-encoded and found in most staphylococcal strains, with a given species producing PSMs of usually only minor amino acid sequence similarity to PSMs of other species (16). Mutants in the quorum-sensing system Agr lack PSM production, because *psm* operon transcription is under strict control by the AgrA DNA binding protein (14, 17, 18). Most work on PSMs has been performed in *S. epidermidis* and *S. aureus*. *S. aureus* produces four PSMα peptides, which are encoded in the *psmα* operon, two PSMβ peptides encoded in the *psmβ* operon, and the RNAIII-encoded δ-toxin (14). The *S. aureus* PSMα peptides and the δ-toxin belong to the group of short α-type PSMs (∼20–25 aa), whereas the PSMβ peptides belong to the β-type PSMs, which are about double in size compared with α-type PSMs.

Here, we hypothesized that members of the PSM peptide family mediate biofilm-structuring processes and biofilm detachment in *S. aureus*, owing to their surfactant-like physicochemical characteristics. To evaluate that hypothesis, we determined the impact of all *S. aureus* PSM peptides on biofilm development. We examined biofilm structure in detail using deletion mutants, high-resolution imaging of biofilm development with confocal laser-scanning microscopy (CLSM), and in-depth mathematical analysis of biofilm parameters. Furthermore, we investigated the impact of PSMs on
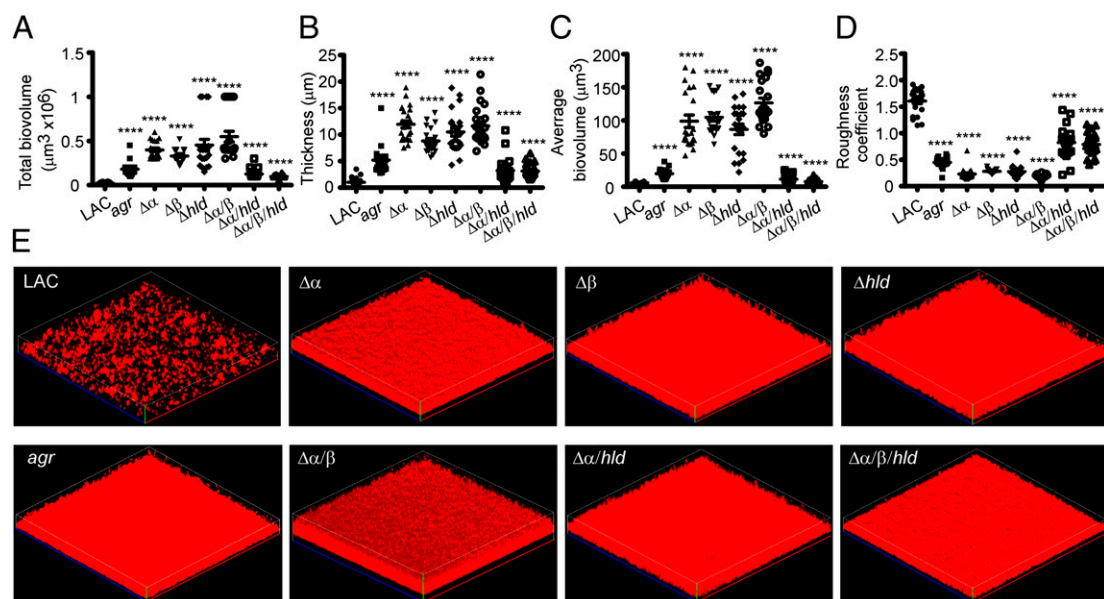

MICROBIOLOGY

Fig. 1. Impact of PSMs and Agr on the structuring of static *S. aureus* biofilms. Static biofilms were grown in eight-well chambered coverglass plates for 48 h. (*A–D*) Biofilm parameters were measured in at least 20 randomly chosen biofilm CLSM images of the same extension. Horizontal bars depict the mean. Statistical analysis is by *t* tests vs. the corresponding values of the WT samples, which were grown and measured separately for every mutant comparison. Only one WT analysis is shown for brevity; however, statistical analysis was performed vs. the corresponding WT samples grown in parallel, which were very similar in all cases. ****$P < 0.0001$. Values for 24-h biofilms were also measured, and differences were similar. (*E*) Example 48-h CLSM biofilm images. Extensions and scales are the same in every image (total *x* extension, 230 μm; total *y* extension, 230 μm).

the dissemination of biofilm-associated infection in a mouse catheter infection model. Our results show that all PSM peptides produced by *S. aureus* impact biofilm structuring, detachment, and in vivo dissemination, and they indicate that PSMs form the major force facilitating those processes. Importantly, our study provides detailed evidence for a key function of surfactant molecules in bacterial biofilm maturation.

Results

To analyze *S. aureus* biofilm maturation processes, we chose the community-associated methicillin-resistant *S. aureus* strains USA300 [Los Angeles County clone (LAC)] and USA400 (MW2) owing to their clinical importance (19, 20), proven involvement in biofilm-associated infections such as osteomyelitis (21) and endocarditis (22), and previously shown dependence of biofilm detachment on the PSM regulator Agr (23). In a preliminary test aimed to determine whether *S. aureus* PSM peptides are biofilm-active, we added synthetic PSM peptides at different concentrations to growing biofilms of a LAC *agr* mutant (lacking intrinsic PSM production). Most PSM peptides inhibited biofilm formation at concentrations exceeding 50 μg/mL with slightly different potencies (Fig. S1). This experiment, thus, established general biofilm activity of *S. aureus* PSM peptides; however, it only gave limited insight into the role of PSMs during biofilm development, because PSMs were added externally and not produced during biofilm growth. In the following experiments, we, therefore, compared biofilms of isogenic *psm* mutants with biofilms of the corresponding WT strains using CLSM, allowing a much better evaluation of the contribution of PSMs to biofilm-structuring processes.

Biofilm formation is commonly analyzed using static or dynamic (flow cell-grown) biofilms. It is debatable which method better reflects in vivo conditions, especially because these conditions may be strongly divergent. Therefore, we analyzed biofilms in both static and dynamic systems. In static biofilms, total biofilm volume and mean thickness values were significantly higher in the *agr* and all *psm* mutants compared with those values

of the WT strain (Fig. 1 *A* and *B* and Fig. S2 *A* and *B*). These results showed that the expansion of static biofilms in *agr* mutants of *S. aureus* that we previously described (5) is, to a large extent, a consequence of lacking expression of PSMs. Furthermore, values of average biofilm volume (a readout of the degree of channel formation) were higher in all mutants compared with the WT (Fig. 1*C* and Fig. S2*C*). In contrast, roughness coefficients were lower, showing that mutant biofilms were smoother than the biofilm formed by the WT strain (Fig. 1*D* and Fig. S2*D*). Similarly, on visual evaluation of representative biofilm images, mutant biofilms appeared more compact, thicker, and smoother on the surface (Fig. 1*E* and Fig. S2*E*). Importantly, these data indicate that (*i*) Agr not only controls biofilm detachment as previously shown (6) but also biofilm structuring and (*ii*) PSMs represent key molecular factors contributing to biofilm structuring and detachment in *S. aureus*. Furthermore, all PSMs of
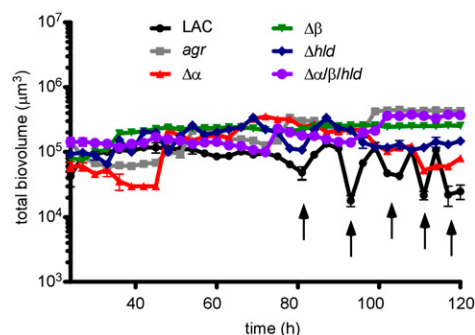

Fig. 2. PSMs are responsible for quorum-sensing controlled waves of detachment in dynamic *S. aureus* biofilms. Dynamic (flow cell) biofilm formation was measured over 5 d, and three randomly chosen biofilm CLSM images were analyzed for the total biovolume at regular intervals. Arrows mark the detachment waves occurring in the WT sample after the third day of biofilm formation.
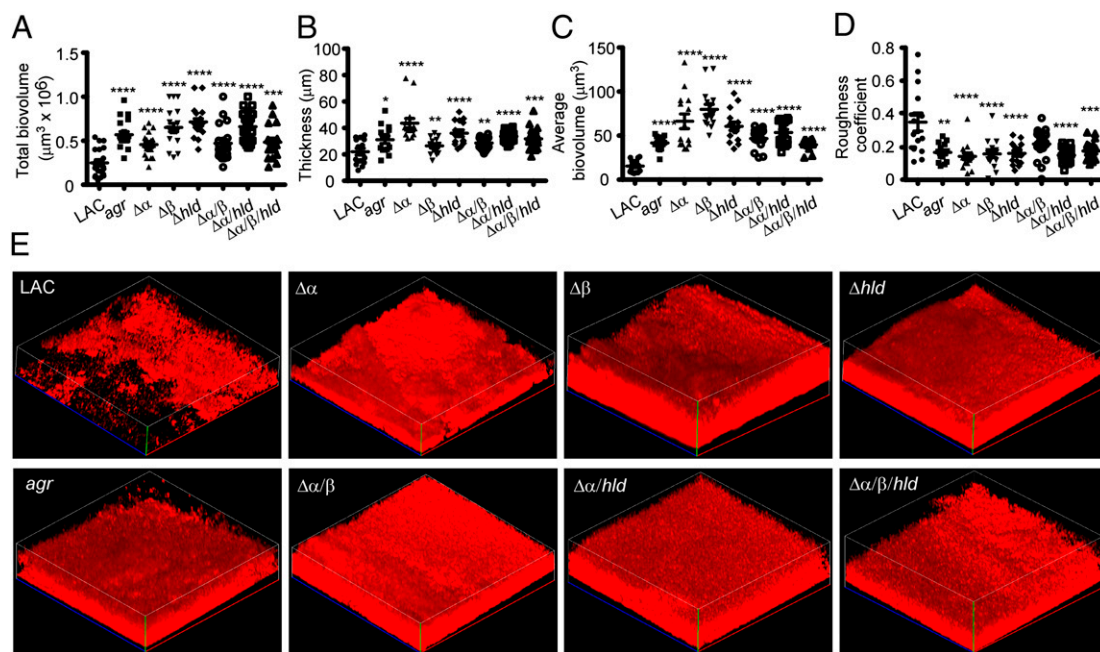
Fig. 3. Impact of PSMs and Agr on the structuring of dynamic (flow cell) *S. aureus* biofilms. Dynamic (flow cell) biofilms were grown for 72 h. (*A–D*) Biofilm parameters were measured at 72 h in at least 14 randomly chosen biofilm CLSM images of the same extension. Horizontal bars depict the mean. Statistical analysis is by *t* tests vs. the corresponding values of the WT samples, which were grown and measured separately for every mutant comparison. Only one WT analysis is shown for brevity; however, statistical analysis was performed vs. the corresponding WT samples grown in parallel, which were very similar in all cases. *P < 0.05; **P < 0.01; ***P < 0.001; ****P < 0.0001. Values for 24- and 48-h biofilms were also measured, and differences were similar. (*E*) Example 48-h CLSM biofilm images. Extensions and scales are the same in every image (total *x* extension, 230 μm; total *y* extension, 230 μm).

S. aureus, PSMα peptides, PSMβ peptides, and the δ-toxin contributed to these processes.

Next, we determined the impact of Agr and PSMs on biofilm development under dynamic conditions using flow cells. Biofilm development was measured over 5 d. After about 72 h, the USA300 WT strain showed the previously described (6) characteristic waves of detachment and regrowth (Fig. 2). Remarkably, no *psm* or *agr* mutant showed this behavior, or it was strongly reduced. In addition, similar to the results obtained with static biofilms, total and average biovolumes and mean thickness values of biofilms were significantly increased in all mutants compared with the WT strains (Fig. 3 *A–D* and Fig. S3 *A–D*), and representative images confirmed the mathematical evaluation on visual examination (Fig. 3*E* and Fig. S3*E*). Of note, we ascertained that the observed effects were not caused by spontaneously occurring mutations in the *agr* or *psm* operons by verifying maintained PSM expression of randomly picked clones of matured biofilms in all strains. Furthermore, induction of expression of the *psmα* or *psmβ* loci or the *hld* gene in a preformed biofilm of a USA300 *psm* triple mutant (Δα/β/*hld*) led to significant decreases in total and average biovolumes in all cases (Fig. 4). These results confirmed the results obtained using static biofilm formation, showing that PSMs are major molecular effectors of Agr-controlled biofilm structuring and detachment in *S. aureus* and that all *S. aureus* PSMs participate in those processes.

To gain additional insight into how the biofilm structure develops on a molecular level, we determined the spatial and temporal arrangement of *agr* and *psm* expression in static and dynamic biofilms using *egfp* fusions of all *psm* gene promoters (*agr*P3, *psmα*, and *psmβ*). In addition, we determined the activity of the *agr*P2 promoter-driving expression of the AgrA DNA binding protein that binds to and controls activities of the *psmα* and *psmβ* promoters (18) (Fig. 5*A*). Expression in biofilms was limited to specific cells and cell clusters for all promoters (Fig. 5 *B–D*). This observation is consistent with the notion that Agr

control and PSM expression drive biofilm structuring inasmuch as this process requires a nonuniform expression of biofilm-
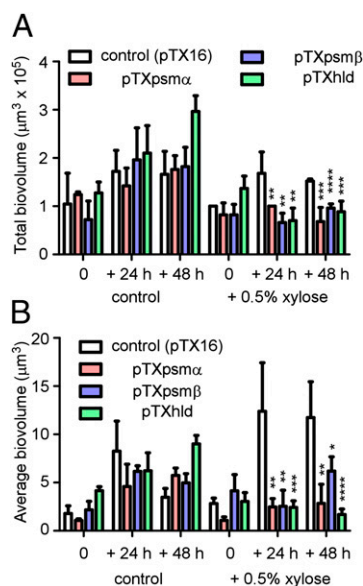

Fig. 4. Induction of PSM expression leads to biofilm detachment in dynamic *S. aureus* biofilms. Dynamic biofilms of the LAC *psm* triple mutant (Δα/Δβ/Δ*hld*) harboring the indicated plasmids were grown in flow cells for 24 h (*t* = 0) in tryptic soy broth without glucose. Then, expression of the respective *psm* genes, which were cloned in the pTX series of plasmids under a xylose-inducible promoter (see Table S1 for all oligonucleotides used), was induced by switching the media to tryptic soy broth without glucose/0.5% xylose. In control samples, the media were not switched. (*A*) Total and (*B*) average biovolumes were measured at 24 and 48 h after in five randomly chosen biofilm CLSM images of the same extension. *P < 0.05; **P < 0.01; ***P < 0.001; ****P < 0.0001; *t* tests vs. corresponding control (pTX16) samples.
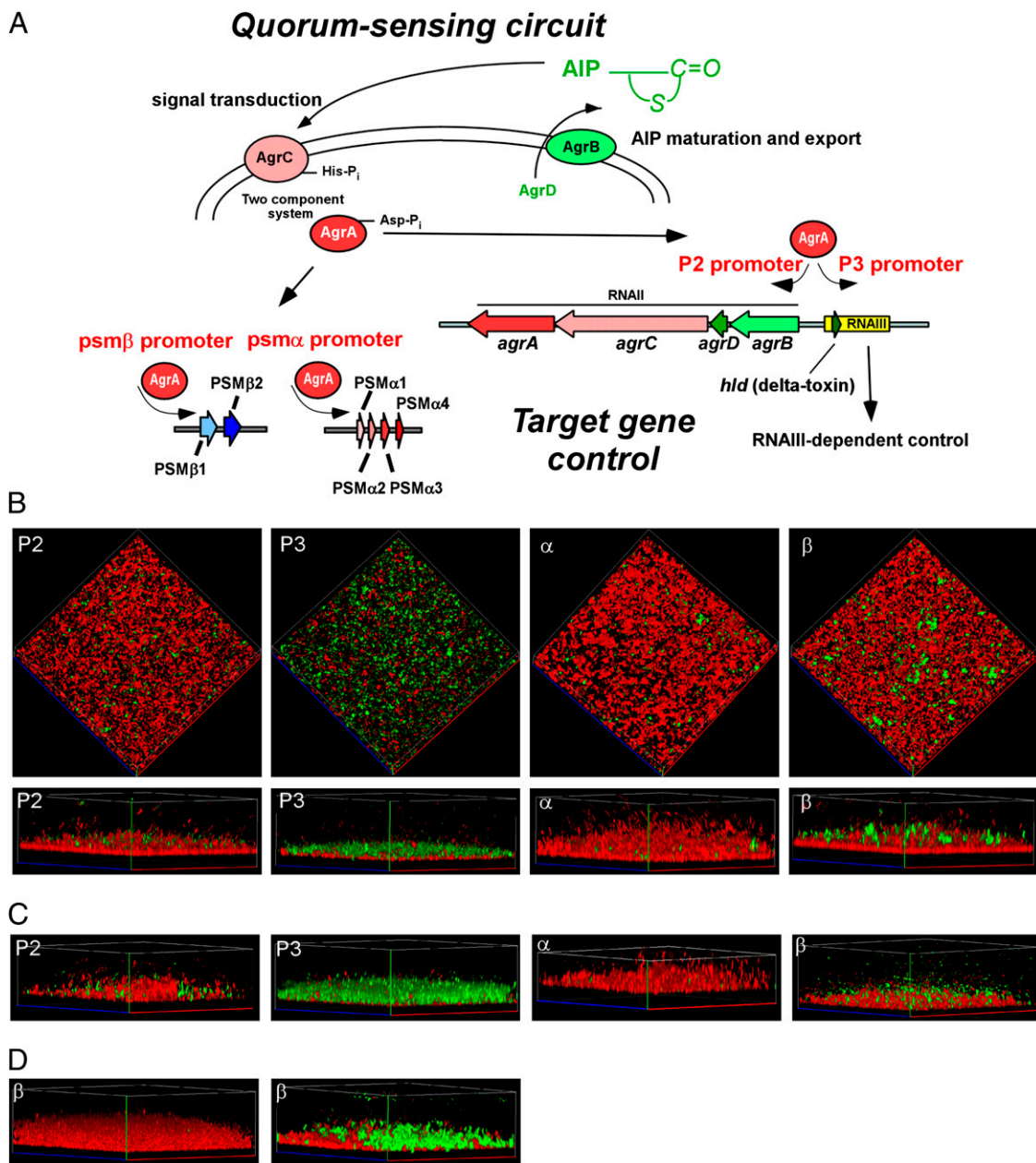
Fig. 5. Expression of *psm* and *agr* promoters in static and dynamic *S. aureus* biofilms. (*A*) Agr quorum-sensing control circuit and regulation of target genes. Modified from ref. 18. The quorum-sensing circuit is shown at the top. AgrB modifies and exports the AgrD Agr autoinducing peptide precursor, which activates the histidine kinase AgrC. Activated (phosphorylated) AgrA binds to the P2, P3, *psmα*, and *psmβ* promoters. The P2 promoter controls expression of RNAII, comprising the *agrB*, *agrD*, *agrC*, and *agrA* transcripts, which form the basis of the Agr quorum-sensing autofeedback mechanism. Most Agr targets other than the *psm* genes are regulated by the P3-controlled RNAIII, which also encodes the PSM δ-toxin (*hld* gene). (*B–D*) CLSM visualization of promoter expression in (*B*) static and (*C* and *D*) dynamic biofilms using promoter-*egfp* transcriptional fusions in strain LAC; *x* and *y* axes dimensions are 160 × 160 μm in all images. In *B*, top and side views are shown of corresponding images. In *C*, example images are shown that depict typical average promoter expression observed for the respective promoters; at different time points or locations in the biofilm, promoter expression was strongly different, which is shown as an example for the *psmβ* promoter in *D*.

structuring factors. Accordingly, although overall expression of the four promoters was comparable between static and dynamic biofilms (Fig. 5 *B* and *C*), there were strong differences in temporal and spatial expression in flow cell biofilms (shown as an example for the *psmβ* promoter in Fig. 5*D*). Furthermore, although *psm* and *agr* promoter expression occurred throughout the biofilm as needed for channel formation, it was strongest in exposed parts of the biofilm in keeping with the idea that cell–cell disruptive forces are highest at the outer levels to control

biofilm expansion. Together, these observations suggest that slight differences in the microenvironment, causing differences in local Agr autoinducing peptide concentration and consequently, Agr activity, underlie the formation of the characteristic biofilm structure through differential Agr-controlled PSM production. Although our findings, thus, indicate that biofilm development depends on the divergent spatial and temporal expression of *agr* and *psm* promoters in biofilm cells, analysis of PSM concentrations in flow cell effluents showed that PSM production in the

entire biofilm relative to the biovolume is constant over time (Fig. S4), which is in accordance with the idea that PSM production is linked to the maintenance of biofilm homeostasis.

Finally, we used a mouse catheter infection model to determine the impact of *S. aureus* PSMs on the dissemination of biofilm-associated infection in vivo. This model was performed as previously described for *S. epidermidis* (4) but not in a competitive mode because of the number of different mutants to be analyzed. Despite noncompetitive models being generally less discriminatory, we detected significantly decreased dissemination of the *psm* triple deletion mutant strain (Δα/β/*hld*) to the catheter-surrounding tissue, adjacent skin, and lymph nodes compared with the WT strain (Fig. 6). Single *psm* mutant strains showed significantly decreased dissemination in at least one of the tested samples. Although these findings are in accordance with our in vitro results indicating that all *S. aureus* PSMs contribute to biofilm detachment, it is likely that, at least for the PSMα peptides, the observed phenotype is influenced in addition by the cytolytic properties of those peptides (14). Of note, the phenotype of the *psm* triple deletion mutant was very similar to the phenotype of the *agr* mutant, underscoring that the failure of *S. aureus agr* mutants to disseminate from a biofilm-infected catheter is largely because of the lack of PSM expression.

Discussion

Our results identify PSMs as key contributors to *S. aureus* biofilm maturation processes, specifically the formation of the characteristic, channel-containing biofilm structure, biofilm detachment, control of biofilm expansion, and dissemination from biofilms in vivo. Furthermore, our findings are in support of a model in which biofilm structuring is dependent on local differences in biofilm maturation factor (PSM) expression, which is driven by variation of quorum-sensing (Agr) activity.

Importantly, these findings significantly expand our knowledge about PSMβ-based dissemination of biofilm-associated infection that we obtained previously in *S. epidermidis* (4). Not only does the present study provide a far more detailed assessment of biofilm maturation processes using in-depth mathematical analysis, it also shows that all PSM classes are biofilm-active and contribute to biofilm structuring and in vivo dissemination. However, it is interesting that the PSMβ peptides in particular showed a pronounced impact on *S. aureus* biofilm structuring, despite much lower concentrations compared with other PSMs and *S. epidermidis* biofilms (4). Promoter expression studies revealed a relatively strong expression of the *psmβ* promoter in *S. aureus* biofilms, suggesting that analyses of PSM concentrations
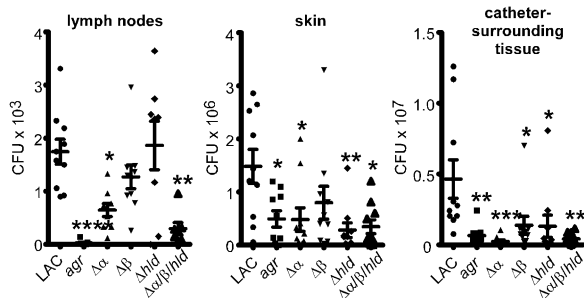
in biofilm cultures or effluents may not adequately reflect PSMβ production in microenvironments. Nevertheless, expression of the *psmβ* promoter was still much lower than expression of the P3 promoter controlling expression of the δ-toxin. Thus, these observations indicate an especially important role of PSMβ among PSM peptides in biofilm maturation. This finding is particularly noteworthy, because production of the noncytolytic PSMβ peptides may enable the bacteria to structure biofilms without aggressive interaction with the host and strong activation of host defense mechanisms, which is likely why they seem to play a more central role in *S. epidermidis* compared with the more aggressive *S. aureus* (24). In that regard, it was interesting that we did not find substantial differences in the pattern of PSM production in biofilm vs. planktonic culture in *S. aureus* (Fig. S5) in contrast to the relative increase in PSMβ production in biofilms previously observed in *S. epidermidis* (4).

We noted that there was no additive effect of PSM absence in *psm* double and triple compared with single mutants in vitro inasmuch as, for example, the total biovolume was not further increased when more than one PSM or PSM class was absent. In static biofilms, effects observed in *psm* single mutants were even more pronounced than effects in double and triple mutants, although all differences were statistically significant. Possibly, in the absence of most or all PSMs, biofilm maturation processes are too severely impaired for biofilms to develop normally than in the absence of only some PSM peptides. However, effects were very similar in the triple *psm* compared with the *agr* mutant, further underscoring that PSMs are major effectors of the quorum-sensing impact on biofilm maturation processes. In vivo, the contribution of the different PSMs to dissemination seemed additive, possibly as a result of at least the PSMα and δ-toxin having additional properties, such as the capacity to lyse red and white blood cells (14).

We previously noted that Agr negatively controls biofilm formation inasmuch as *agr* mutant strains produced thicker biofilms (5). Our present results mechanistically refine this model by showing that the observed excessive biofilm thickness of *agr* mutants is the result of abnormal biofilm development, which is caused by the lack of PSM-dependent biofilm structuring and control of biofilm expansion. In that regard, it is important to stress that many previous studies on *S. aureus* biofilms were performed in laboratory strains, several of which were Agr-dysfunctional (such as strain SA113) and likely selected because of their extended biofilm thickness. Of note, *agr* mutants are also frequently isolated clinically from biofilm-covered devices, presumably because compact and extended biofilms are of a certain advantage to the bacteria in specific stages of chronic infection (25); notably, however, these strains likely represent a dead end of infection, because they lack the capacity to disseminate within the body (4) or establish infection in other hosts (26).

The presence of quorum-sensing controlled surfactant molecules in several biofilm-forming bacteria (9–12) indicates that the mechanism that we describe here in *S. aureus* represents a widespread mechanism of biofilm structuring. It is possible that enzymes that degrade biofilm polymers provide additional structuring for which there is some recent evidence in *S. aureus* (7, 8); however, how such enzymes contribute to biofilm maturation awaits in-depth investigation. Furthermore, our study suggests that targeting biofilm-structuring surfactant molecules might represent a promising approach to prevent the formation of viable medical and environmental biofilms, although the species-specific chemical nature of these molecules would likely require a specific form of interference in every case.

Methods

CLSM. Static biofilms were grown in eight-well chambered coverglass plates (Lab-Tek) and analyzed on a Zeiss LSM 700 confocal microscope after gentle washing and staining with propidium iodide (10 μM) for 15 min. Dynamic biofilms were grown using Stovall flow cells under a flow of 0.5 mL/min of

Fig. 6. Mouse model of biofilm-associated infection. Two catheter pieces coated with the same strain of USA300 (LAC) WT or isogenic *psm* mutant bacteria (~3 × 10⁵ cfu per catheter piece) were inserted in the left and right dorsum of Nu/Nu mice. At day 7, mice were euthanized, and disseminated bacteria were counted. Samples with considerable bacterial numbers are shown. Only very small numbers of bacteria were found in the organs. *$P <$ 0.05; **$P <$ 0.01; ***$P <$ 0.001; ****$P <$ 0.0001 vs. LAC (one-way ANOVA with Bonferroni posttests).

medium containing 10 μM propidium iodide. The developing biofilms were scanned at regular intervals over the given period (usually 5 d).

Mouse Model of Biofilm-Associated Infection. The model was performed as previously described (4) with the following modifications. One-centimeter pieces of catheter tubing (Terumo Surflash IV catheter, 14 gauge × 2 in, radio opaque, SR*FF1451) were coated for 2 h with bacterial suspensions, resulting in adherence of ~3 × 10^5 cfu; two pieces coated with the same strain or mutant were inserted at the left and right dorsum of Nu/Nu mice, and the incisions were closed with tissue adhesive glue. At day 7 after infection, mice were euthanized, and the tissue surrounding the catheter; the adjacent skin; the inguinal, axillar, brachial, superficial cervical, and lumbar lymph nodes; and the kidneys, spleens, and liver was analyzed for bacteria. Values obtained for all lymph nodes were added; values obtained for the left and right skin, tissue, and organ samples were also added.

Additional detailed protocols are reported in SI Methods.

1. Costerton JW, Stewart PS, Greenberg EP (1999) Bacterial biofilms: A common cause of persistent infections. *Science* 284:1318–1322.
2. Otto M (2008) Staphylococcal biofilms. *Curr Top Microbiol Immunol* 322:207–228.
3. Watnick P, Kolter R (2000) Biofilm, city of microbes. *J Bacteriol* 182:2675–2679.
4. Wang R, et al. (2011) *Staphylococcus epidermidis* surfactant peptides promote biofilm maturation and dissemination of biofilm-associated infection in mice. *J Clin Invest* 121:238–248.
5. Vuong C, Saenz HL, Götz F, Otto M (2000) Impact of the *agr* quorum-sensing system on adherence to polystyrene in *Staphylococcus aureus. J Infect Dis* 182:1688–1693.
6. Yarwood JM, Bartels DJ, Volper EM, Greenberg EP (2004) Quorum sensing in *Staphylococcus aureus* biofilms. *J Bacteriol* 186:1838–1850.
7. Boles BR, Horswill AR (2008) Agr-mediated dispersal of *Staphylococcus aureus* biofilms. *PLoS Pathog* 4:e1000052.
8. Mann EE, et al. (2009) Modulation of eDNA release and degradation affects *Staphylococcus aureus* biofilm maturation. *PLoS One* 4:e5822.
9. Branda SS, González-Pastor JE, Ben-Yehuda S, Losick R, Kolter R (2001) Fruiting body formation by *Bacillus subtilis. Proc Natl Acad Sci USA* 98:11621–11626.
10. Angelini TE, Roper M, Kolter R, Weitz DA, Brenner MP (2009) *Bacillus subtilis* spreads by surfing on waves of surfactant. *Proc Natl Acad Sci USA* 106:18109–18113.
11. Davey ME, Caiazza NC, O'Toole GA (2003) Rhamnolipid surfactant production affects biofilm architecture in *Pseudomonas aeruginosa* PAO1. *J Bacteriol* 185:1027–1036.
12. Boles BR, Thoendel M, Singh PK (2005) Rhamnolipids mediate detachment of *Pseudomonas aeruginosa* from biofilms. *Mol Microbiol* 57:1210–1223.
13. Mehlin C, Headley CM, Klebanoff SJ (1999) An inflammatory polypeptide complex from *Staphylococcus epidermidis*: Isolation and characterization. *J Exp Med* 189:907–918.
14. Wang R, et al. (2007) Identification of novel cytolytic peptides as key virulence determinants for community-associated MRSA. *Nat Med* 13:1510–1514.
15. Cheung GY, et al. (2010) *Staphylococcus epidermidis* strategies to avoid killing by human neutrophils. *PLoS Pathog* 6:e1001133.
16. Rautenberg M, Joo HS, Otto M, Peschel A (2011) Neutrophil responses to staphylococcal pathogens and commensals via the formyl peptide receptor 2 relates to phenol-soluble modulin release and virulence. *FASEB J* 25:1254–1263.
17. Vuong C, et al. (2004) Regulated expression of pathogen-associated molecular pattern molecules in Staphylococcus epidermidis: Quorum-sensing determines pro-inflammatory capacity and production of phenol-soluble modulins. *Cell Microbiol* 6:753–759.
18. Queck SY, et al. (2008) RNAIII-independent target gene control by the *agr* quorum-sensing system: Insight into the evolution of virulence regulation in *Staphylococcus aureus. Mol Cell* 32:150–158.
19. Moran GJ, et al. (2006) Methicillin-resistant *S. aureus* infections among patients in the emergency department. *N Engl J Med* 355:666–674.
20. CDC (1999) From the Centers for Disease Control and Prevention. Four pediatric deaths from community-acquired methicillin-resistant *Staphylococcus aureus*—Minnesota and North Dakota, 1997–1999. *JAMA* 282:1123–1125.
21. McCaskill ML, et al. (2007) Increase of the USA300 clone among community-acquired methicillin-susceptible *Staphylococcus aureus* causing invasive infections. *Pediatr Infect Dis J* 26:1122–1127.
22. Haque NZ, et al. (2007) Infective endocarditis caused by USA300 methicillin-resistant *Staphylococcus aureus* (MRSA). *Int J Antimicrob Agents* 30:72–77.
23. Lauderdale KJ, Malone CL, Boles BR, Morcuende J, Horswill AR (2010) Biofilm dispersal of community-associated methicillin-resistant Staphylococcus aureus on orthopedic implant material. *J Orthop Res* 28:55–61.
24. Otto M (2009) *Staphylococcus epidermidis*—the 'accidental' pathogen. *Nat Rev Microbiol* 7:555–567.
25. Traber KE, et al. (2008) *agr* function in clinical *Staphylococcus aureus* isolates. *Microbiology* 154:2265–2274.
26. Shopsin B, et al. (2010) Mutations in *agr* do not persist in natural populations of methicillin-resistant *Staphylococcus aureus. J Infect Dis* 202:1593–1599.